Electronic supplementary information

Plasmonic CuS Nanodisk Assemblies Based Composite Nanocapsules for NIR-Laser-Driven Synergistic Chemo-Photothermal Cancer Therapy

Jian He, [a, ‡] Xin Liu, [b, ‡] Lisha Ai, [c, ‡] Hao Huang, [a,*] Yuebin Li,[a,*] Mingguang Zhang,[a] Qianru Zhao,[a] Xingguo Wang,[b] Wei Chen [d] and Haoshuang Gu[a,*]

[a]Hubei Collaborative Innovation Center for Advanced Organic Chemical Materials—Hubei Key Laboratory of Ferro & Piezoelectric Materials and Devices, Faculty of Physics & Electronic Sciences, Hubei University, Wuhan 430062, China.
[b]Faculty of Life Sciences, Hubei University, Wuhan 430062, China.
[c]Institute of Hematology, Union Hospital, Tongji Medical College, Huazhong University of Science and Technology, Wuhan 430022, China
[d]Department of Physics, The University of Texas at Arlington, Arlington, TX 76019-0059, USA.
*Email - ybli@hubu.edu.cn, davidleenanoc@gmail.com

1. Calculation of the photothermal conversion efficiency of Au nanorods

The photothermal conversion efficiency (η) of CTAB decorated Au nanorods with an average size of 85×15 nm derived by TEM image (Figure S4a) was measured by applying an energy balance to obtain a microscale heat-transfer time constant from the transient temperature profile (Figure S4c) by using the following Equations according to the previous report.[1] In the equation, h and S are the heat transfer coefficient and the surface area of the container, respectively, and

$$\eta = \frac{hS(T_{Max} - T_{Surr}) - Q_{Dis}}{I(1 - 10^{-A_{980}})} \quad (1)$$

$$hS = \frac{m_D C_D}{\tau_s} \quad (2)$$

$$\theta = \frac{T - T_{Surr}}{T_{Max} - T_{Surr}} \quad (3)$$

$$t = -\tau_s \ln(\theta) \quad (4)$$

the value of hS is obtained from Equation (2) and Figure S4d. The maximum steady temperature (T_{Max}) was 48.3 °C and environmental temperature (T_{Surr}) was 25.0 °C. Correspondingly,

$Q_{Dis}=hS(T_{Max,Water}-T_{Surr,Water})$ which is heat dissipated from the light absorbed by the solvent and container. The laser power (I) is 0.385 W. A_{980} is the absorbance of Au nanorods at 980 nm which in this case was chosed to be 6 (the maximum of our instrument) (in Figure S4b). A dimensionless parameter θ and a sample system time constant can be calculated as Equation (3) and Equation (4). According to Figure S4d, τ_s was determined and calculated to be 284.25 s. Moreover, the mass of sample (m_D) is 0.3 g and the thermal capacity of sample (C_D) is $4.2\ \mathrm{J}/g.°C$. Thus, according to Equation 2, hS is calculated to be $4.43\ \mathrm{mW}/°C$. Similarly, $Q_{Dis}=hS(T_{Max,Water}-T_{Surr,Water})$ was determined independently to be 13 mW. Thus, according to Equation (1), the photothermal conversion efficiency (η) of the Au nanorods at 980 nm can be calculated to be 23.4 %.

2.Supplementary Figures

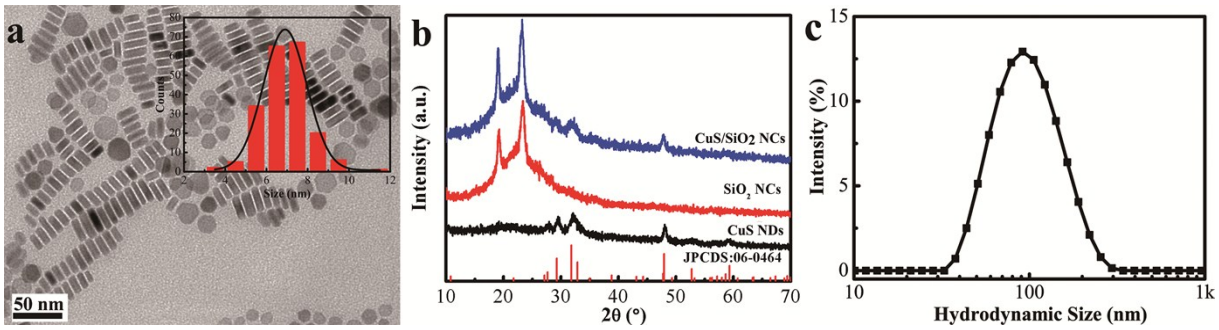

Figure S1. a) TEM images of CuS NDs assembled face-to-face on the pure carbon-coated copper mesh grid The inset shows corresponding height distribution of CuS nanodisks depended by TEM. b) XRD patterns of CuS nanodisks, SiO_2 NCs, and CuS/SiO_2 NCs. c) Hydrodynamic size distribution of CuS /SiO_2 NCs measured by DLS.

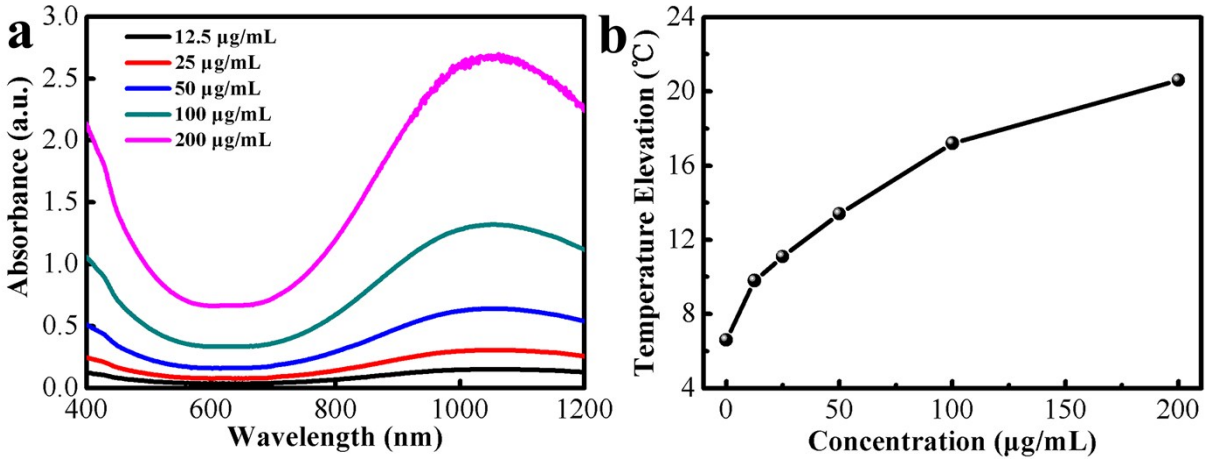

Figure S2. a) UV-Vis-NIR absorbance spectra of CuS/SiO_2 nanocapsules dispersed in water with varied concentrations. b) Plot of temperature elevation over a period of 300 s versus the concentration of the CuS under the irradiation of 980 nm laser with power density of 1.0 W cm^{-2}.

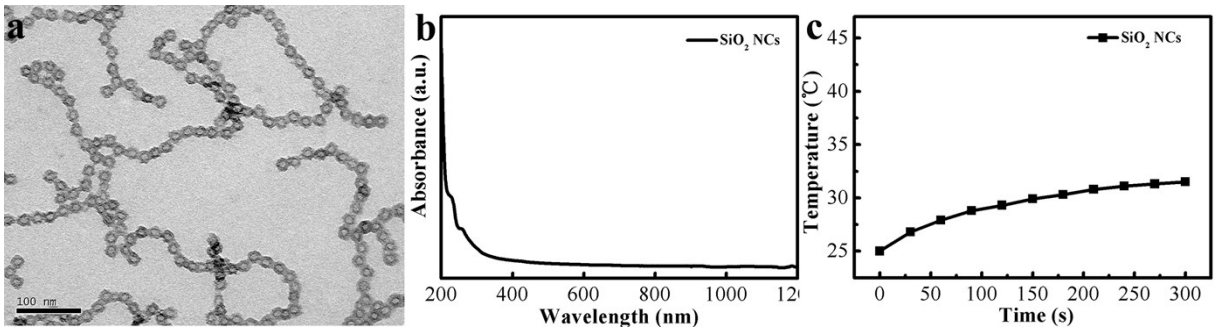

Figure S3. Photothermal properties of SiO_2 NCs. a) TEM images of SiO_2 NCs b) UV-Vis-NIR absorbance spectra of SiO_2 NCs in DI water. c) Temperature evolution of SiO_2 NCs solution under irradiation with a 980-nm laser (1.0 W cm^{-2}).

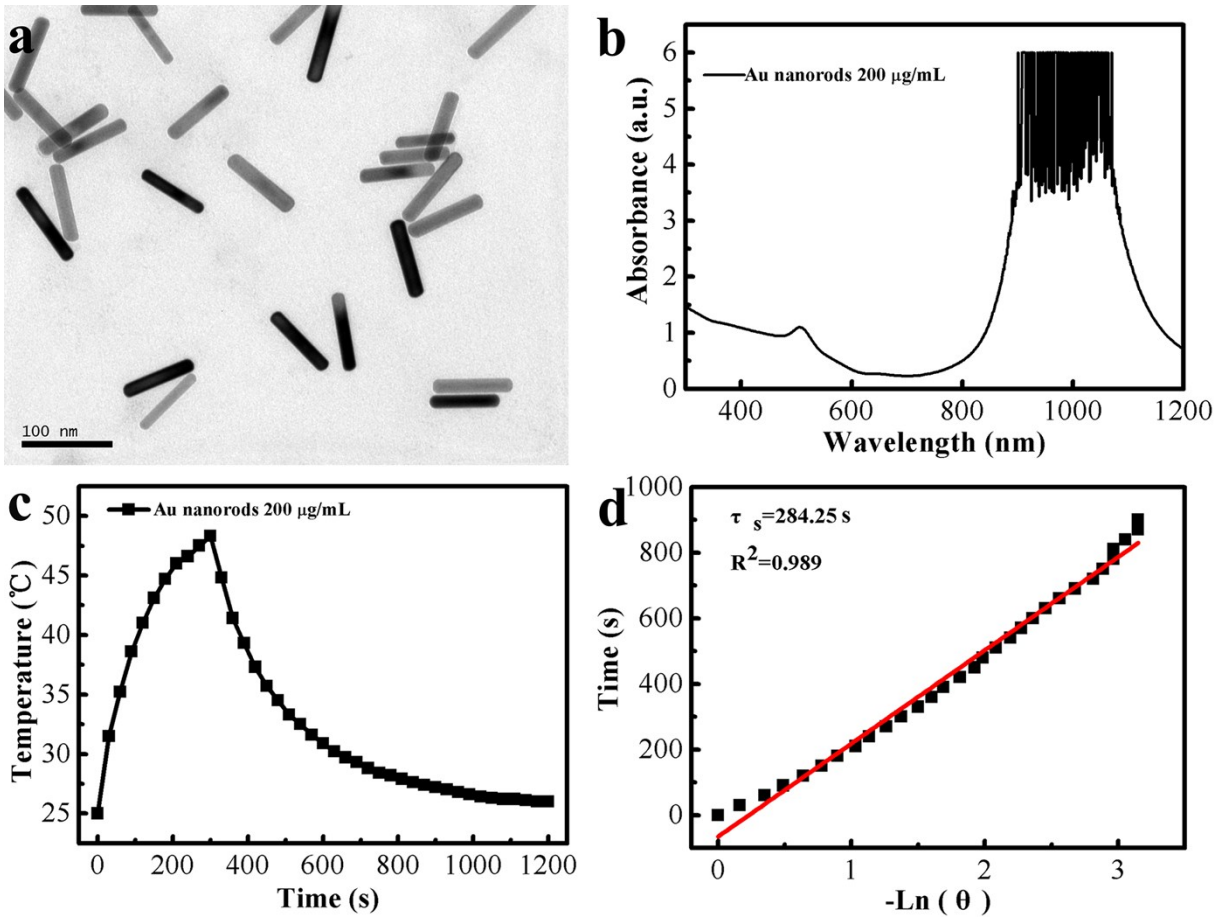

Figure S4. Photothermal properties of Au nanorods. a) TEM images of Au nanorods b) UV-Vis-NIR absorbance spectra of Au nanorods (200 μg mL^{-1}) in DI water. c) Temperature evolution of Au nanorods (200 μg mL^{-1}) solution under irradiation with a 980-nm laser (1.0 W cm^{-2}) d) Linear time data versus -ln(θ) obtained from the cooling period of c).

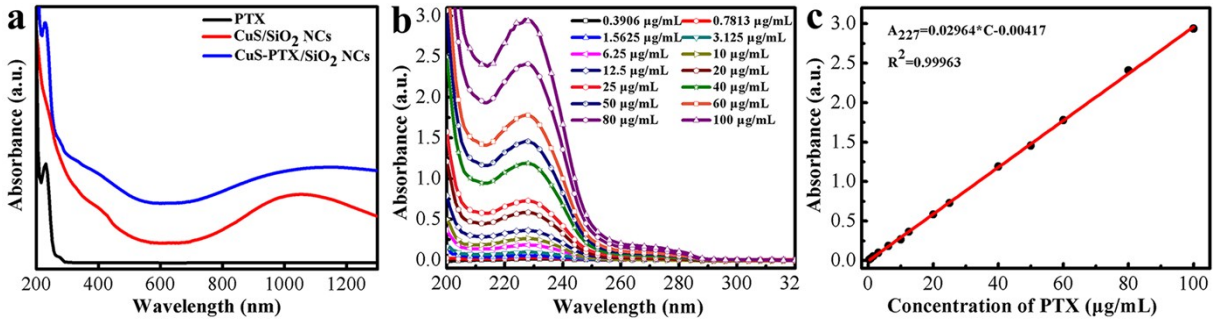

Figure S5. a) UV-Vis-NIR absorbance spectra of PTX/SiO_2 NCs, CuS/SiO_2 NCs, CuS-PTX/SiO_2 NCs. b) UV-Vis-NIR absorbance spectra of PTX dispersed in Acetonitrile with different concentrations. c) Plots of linear fitted absorbance at 227 nm versus the concentration of PTX.

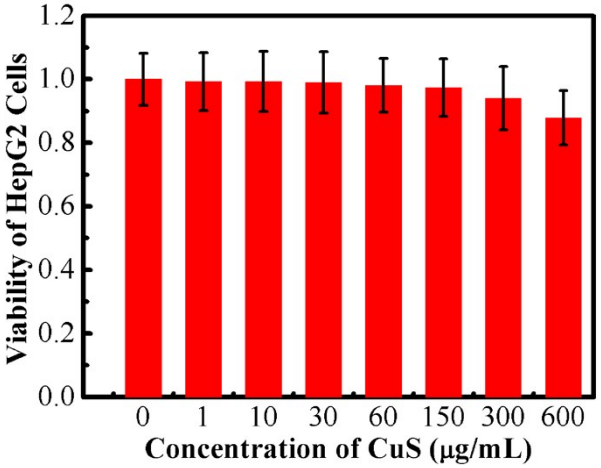

Figure S6. Viability of the HepG2 cells cultured with CuS/SiO_2 NCs with varied concentration up to 600 μg mL^{-1} for 24 h.

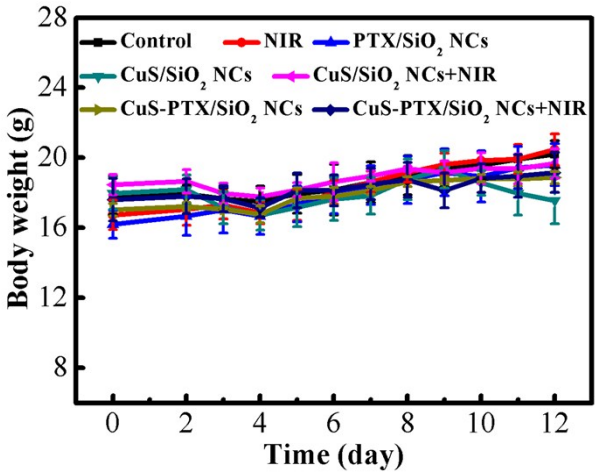

Figure S7. Body weight evolution of different groups by treatment of PBS (control), PBS and laser (NIR), PTX/SiO_2 nanocapsules (PTX/SiO_2 NCs), CuS/SiO_2 nanocapsules (CuS/SiO_2 NCs), CuS nanocapsules with laser (CuS/SiO_2 NCs+NIR), CuS-PTX/SiO_2 nanocapsules (CuS-PTX/SiO_2 NCs) and CuS-PTX with laser (CuS-PTX /SiO_2 NCs+NIR).

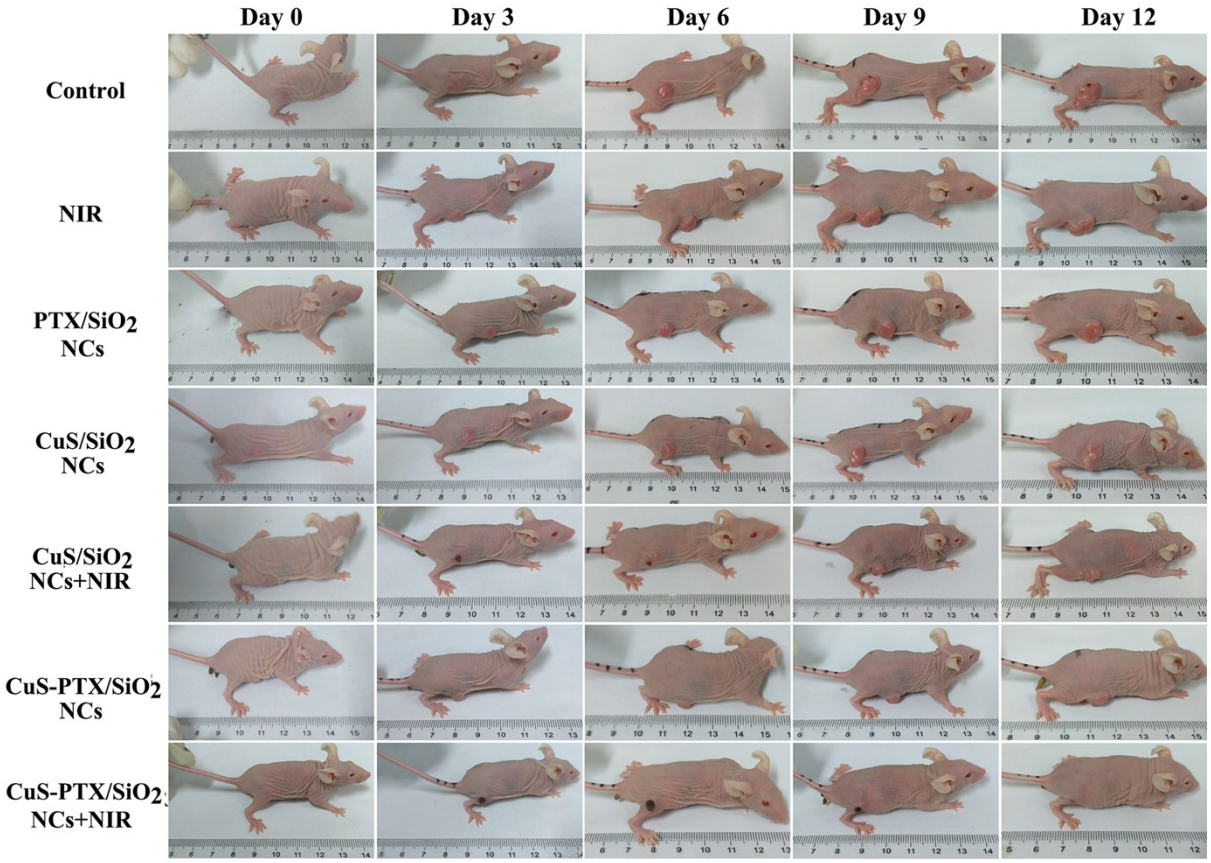

Figure S8. Photographs of mice in different groups before and 12 days after treatment.

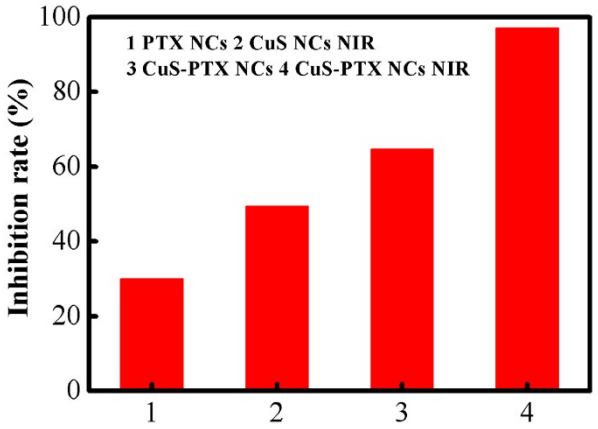

Figure S9. The tumor inhibition rate of different group HepG2 tumor-bearing BALB/c-nu mice treated with nanocapsules and NIR laser.

3. Reference

1. Roper, D. K.; Ahn, W.; Hoepfner, M. *J. Phys. Chem. C* **2007**, 111, 3636-3641.